Biosensors and Bioelectronics 188 (2021) 113270

Contents lists available at ScienceDirect

Biosensors and Bioelectronics

journal homepage: www.elsevier.com/locate/bios

A thread-based wearable sweat nanobiosensor

Chen Zhao [a], Xiao Li [b,c], Qiyang Wu [a,b], Xinyu Liu [a,d,*]

[a] Department of Mechanical & Industrial Engineering, University of Toronto, Canada
[b] Department of Mechanical Engineering, McGill University, Canada
[c] State Key Laboratory for Manufacturing Systems Engineering, Xi'an Jiaotong University, China
[d] Institute of Biomedical Engineering, University of Toronto, Canada

ARTICLE INFO

Keywords:
Wearable biosensor
e-textile
Sweat testing
Lactate
Sodium
Zinc-oxide nanowire

ABSTRACT

Non-invasive wearable biosensors provide an efficient way of continuously quantifying a person's biochemical parameters, and are highly valuable for predicting human physiological status and flagging risks and illness. Commercial wearable sensors are available for tracking a user's physical activities, but few could monitor user's health conditions through sweat analysis. Electronic textile (e-textile) biosensors enable new applications in this scenario because of its high flexibility/wearability, low cost, high level of electronic integration, and unobtrusiveness. However, challenges in developing e-textile sweat biosensors remain in the production of textile-based biosensing materials, skin interfacing design, and embedded data acquisition/transmission. Here, we propose a novel wearable electrochemical sweat biosensor based on conductive threads decorated with zinc-oxide nanowires (ZnO NWs) and apply it to detecting lactate and sodium in perspiration during physical exercise. The sweat biosensor is fully integrated with signal readout and data communication circuits in a wearable headband and is capable of monitoring human sweat accurately and wirelessly. We achieved the detection of lactate and sodium in linear ranges of 0–25 mM and 0.1–100 mM and limits of detection of 3.61 mM and 0.16 mM, respectively, which cover the clinically-relevant ranges of lactate and sodium in human sweat. We demonstrated accurate lactate and sodium measurements in human sweat from a healthy volunteer, and the results are in good agreement with standard test results. We also conducted on-body measurements on the same human volunteer during exercise and confirmed the robustness of the signal readout during body movements and the excellent accuracy of the testing results.

1. Introduction

Non-invasive wearable sensors provide an efficient way of continuously quantifying information on the person's physical (Lee and Chung, 2009; Zhou et al., 2020), chemical (Mitsubayashi et al., 2003; Sempionatto et al., 2020) and biological (Gao et al., 2016; Yang et al., 2020) variables, and are highly valuable for monitoring people's physiological conditions and flagging risks and illness (Pantelopoulos and Bourbakis, 2010; Seshadri et al., 2019; Windmiller and Wang, 2013; Yu et al., 2020). Commercially available wearable sensors are capable of tracking an individual's physical activities like heart rate, blood pressure, electrocardiogram and skin temperature, but fail to provide insight about the user's health state through biochemical cues (Gao et al., 2016). New types of wearable biosensors have been developed and applied to analysis of body fluids such as saliva (Kim et al., 2015), tear (Iguchi et al., 2007; Yao et al., 2012), and sweat (Alizadeh et al., 2018; Bariya et al., 2018; Gamella et al., 2014; Garcia-Cordero et al., 2018; Kim et al., 2018; Modali et al., 2016; Tai et al., 2018), and the target analytes of these wearable biosensors include chemical and biomarkers like metabolites (Modali et al., 2016; RoyChoudhury et al., 2018), electrolytes (Bandodkar et al., 2014; Guinovart et al., 2013), drug compounds (Tai et al., 2018), and the pH level (Curto et al., 2012; Morris et al., 2009).

Electronic textile (e-textile) biosensors, which are realized by integrating electronic components and functionalities into textile substrates, have emerged as an attractive type of wearable device for on-body biosensing (He et al., 2019; Wang et al., 2021). Due to its ease of fabrication, low cost, high level of electronic integration, and unobtrusiveness, e-textile biosensors have great potential in personal healthcare (Chung et al., 2019; Possanzini et al., 2020). Because of its textile nature, it offers a tight but friendly contact to skin with potential integration with real garments, and thus attracts considerable attentions for on-skin sweat analysis during a user's normal daily activities. In recent years,

* Corresponding author. 5 King's College Rd, Toronto, Ontario, M5S 3G8, Canada.
E-mail address: xyliu@mie.utoronto.ca (X. Liu).

https://doi.org/10.1016/j.bios.2021.113270
Received 30 January 2021; Received in revised form 3 April 2021; Accepted 19 April 2021
Available online 24 April 2021

there arise various e-textile-based wearable platforms for human health monitoring. For instance, Wang et al. developed a stretchable gold fiber-based wearable textile electrochemical biosensor for lactate monitoring in sweat (Wang et al., 2021). Jeerapan et al. reported a stretchable textile-based self-powered biosensor with a printed biofuel cell on the sample substrate, and applied it to lactate sensing on human foot (Jeerapan et al., 2016). Despite these advances, challenges in e-textile sweat wearable biosensors remain in the production of textile-based biosensing materials, skin interfacing design, embedded data readout and wireless transmission, and wearable platform integration (Chung et al., 2019; Guinovart et al., 2013; Koh et al., 2016; Lmberis and Dittmar 2007). Nanomaterial-based textile composites have the potential to significantly surpassing the properties of conventional conductive textile materials (Karuppusamy et al., 2017; Wang et al., 2021; Yilmaz, 2018). In particular, semiconductor zinc oxide nanowires (ZnO NWs) are one type of versatile nanomaterial for biosensing on flexible substrates because of its superior physical and chemical properties such as good biocompatibility, high surface electron transfer rate, and convenient synthesis process (e.g., hydrothermal growth) (Song et al., 2017; Zhang et al., 2012).

Lactate and sodium are the most commonly analyzed markers in sweat and can provide meaningful indicators for many physiological conductions. Sweat lactate is a biochemical indicator of anaerobic metabolism in patients with circulatory failure, with theoretical reflection to glycolytic ATP production supporting sweat formation and secretion in eccrine glands (Buono et al., 2010; Wolfe et al., 1970). Its concentration in sweat increases during physical exercise, making it a useful parameter to monitor people's wellness and fitness strength (Buono et al., 2010). Sweat sodium is an excellent marker for potential electrolyte imbalance during exercise (Bandodkar et al., 2014). Considering the deleterious physiological risks raised by sodium lost, its replenishment is essential for regulating water balance, pH, and osmotic pressure of the body (Bandodkar et al., 2014). Thus, continuous monitoring of sweat lactate and sodium concentrations during exercise is useful for regulating the fitness strength and alerting any risks due to over-exercise. It could help indicate the athlete's electrolyte balance, provide timely information to correct, dehydration, acidosis and electrolyte metabolism disorders. In addition to the monitoring of athletic electrolyte, the dysregulation of lactic acid and sodium ions is also closely related to many specific diseases. The accumulation of lactic acid in the initial stage causes soreness and fatigue (Sahlin, 1986). If left unattended for a long time, it will cause acidification of the body and may cause serious diseases such as lactic acidosis; this may lead to dehydration, deep coma, and even shock (Rachoin et al., 2010). Sweat sodium dysregulation may be related to pancreatic cystic fibrosis (Donaldson and Boucher, 2007), glycogen storage disease (HARRIS and COHEN, 1963), and even respiratory disease (Anderson et al., 1962). Thus, it is of great significance to provide a timely measurement method for the concentrations of lactate and sodium in the sweat.

In this paper, we present a thread-based wearable electrochemical biosensor with ZnO-NW-decorated sensing electrodes, for on-body, simultaneous detection of lactate and sodium ion in sweat during perspiration. The biosensor and its signal readout and transmission circuits were fully integrated into a wearable sweat headband, which can wirelessly communicate with a smartphone for data transmission. ZnO NWs were directly synthesized on thread carbon electrodes through low-temperature hydrothermal growth, and specific sensing membranes were applied to the ZnO-NW electrodes for lactate and sodium ion detection. With the ZnO-NW electrodes, two thread-based electrochemical cells were constructed for attachment to the skin, which generated electrical output signals when the sweat was transported to the sensor during user perspiration. Based on this platform, simultaneous detection of lactate and sodium ion in human sweat were demonstrated with linear ranges of 0–25 mM and 0.1–100 mM and limits of detection (LODs) of 3.61 mM and 0.16 mM, respectively. These values cover the clinically-relevant ranges of the lactate and sodium in human sweat. A real human sweat sample, collected from a healthy donor after 30 min of exercise, was tested for off-body testing. The results were found to be 13.16 ± 0.83 mM for lactate and 92.90 ± 5.00 mM for sodium, both in good agreement with the standard test results. On-body sweat testing was also conducted on the same donor after 5-min intense exercise, which confirms the robustness of the signal readout during body movements and the excellent accuracy of the testing results. This thread-based wearable biosensor could be used for on-body sweat testing during physical activities with the purposes of physiological conduction monitoring and electrolyte imbalance detection.

2. Experimental methods

2.1. Materials and reagents

The thread-based carbon electrode for *in-situ* ZnO-NW growth was constructed using cotton thread (Aunt Lydia size 10, *Walmart*), polydimethylsiloxane (PDMS; Sylgard 184, *Dow Corning*), carbon ink (E3456, *Ercon Inc.*), silver ink (E1660, *Ercon Inc.*) and silver/silver chloride (Ag/AgCl) ink (E2411, *Ercon Inc.*). All the chemical reagents were purchased from Sigma Aldrich Canada and used without further purification. For ZnO-NW hydrothermal growth, the required reagents include zinc acetate dihydrate (ZAD), sodium hydroxide (NaOH), ethanol, zinc nitrate hexahydrate (ZNH), hexamethylenetetramine (HMTA), and ammonium hydroxide (AH). For preparing lactate enzymatic membrane, the required reagents include tetrathiafulvalene (TTF), Nafion™, chitosan, L-lactate oxidase (LO_x) (33 U/mg), and glutaraldehyde. For preparing sodium selective membrane, the required reagents include sodium chloride, selectophore™ grade sodium ionophore X, bis(2-ethylhexyl) sebacate (DOS), sodium tetrakis[3,5-bis (trifluoromethyl)phenyl] borate (Na-TFPB), and polyvinyl chloride (PVC). For preparing the reference electrode (RE) membrane, the required reagents include polyvinyl butyral resin BUTVARs B-98 (PVB), and tetrahydrofuran (THF). Artificial sweat was prepared following the standard recipe in ISO 3160-2, namely 20 g/L NaCl, 17.5 g/L NH_4OH, 5 g/L acetic acid, and 15 g/L lactic acid, with the pH adjusted by NH_4OH to 7.0.

2.2. Overall architecture design

Fig. 1A visualizes the concept of our wearable biosensor design for on-body sweat testing during physical activities. The on-skin biosensor includes two electrochemical cells, both with ZnO-NW-coated sensing electrodes, for enzymatic lactate detection and sodium ion-selective sensing, which simultaneously measure concentrations of the lactate and sodium ion in sweat. The lactate sensing electrode (LSE) and the sodium sensing electrode (SSE) were coated with semiconductor ZnO NWs to improve their surface-area-to-volume ratio, electron transport efficiency, and detection sensitivity. The high surface-to-volume ratios of ZnO NWs could expand the surface of the electrodes involved in the potentiometric measurement of lactate and sodium. In our previous research, we found much higher sensitivity in the enzymatic detection of glucose for electrodes decorated with ZnO NWs than that of non-decorated ones (Li et al. 2015, 2021). Experiments have been performed to explore the relationship between sensitivity and ZnO-NW growth time (thus the ZnO NW length). The sensitivity was improved with longer ZnO NWs, which indicated a larger effective surface area on the working electrode (Li et al., 2021). Besides that, Zn NWs could help immobilize enzymes more efficiently and stably due to their strong electrostatic attraction (Li et al. 2015, 2021).

Potentiometric measurement was employed to quantify the electromotive forces (EMF), as the sensor readouts, produced from the electrochemical enzymatic reaction between lactate and lactate oxidase and the selective sodium ion transport into a sodium-selective electrode. We constructed a 'smart' headband (Fig. 1B and C) with a microcontroller-based circuit for real-time measurement of the EMF signals from the

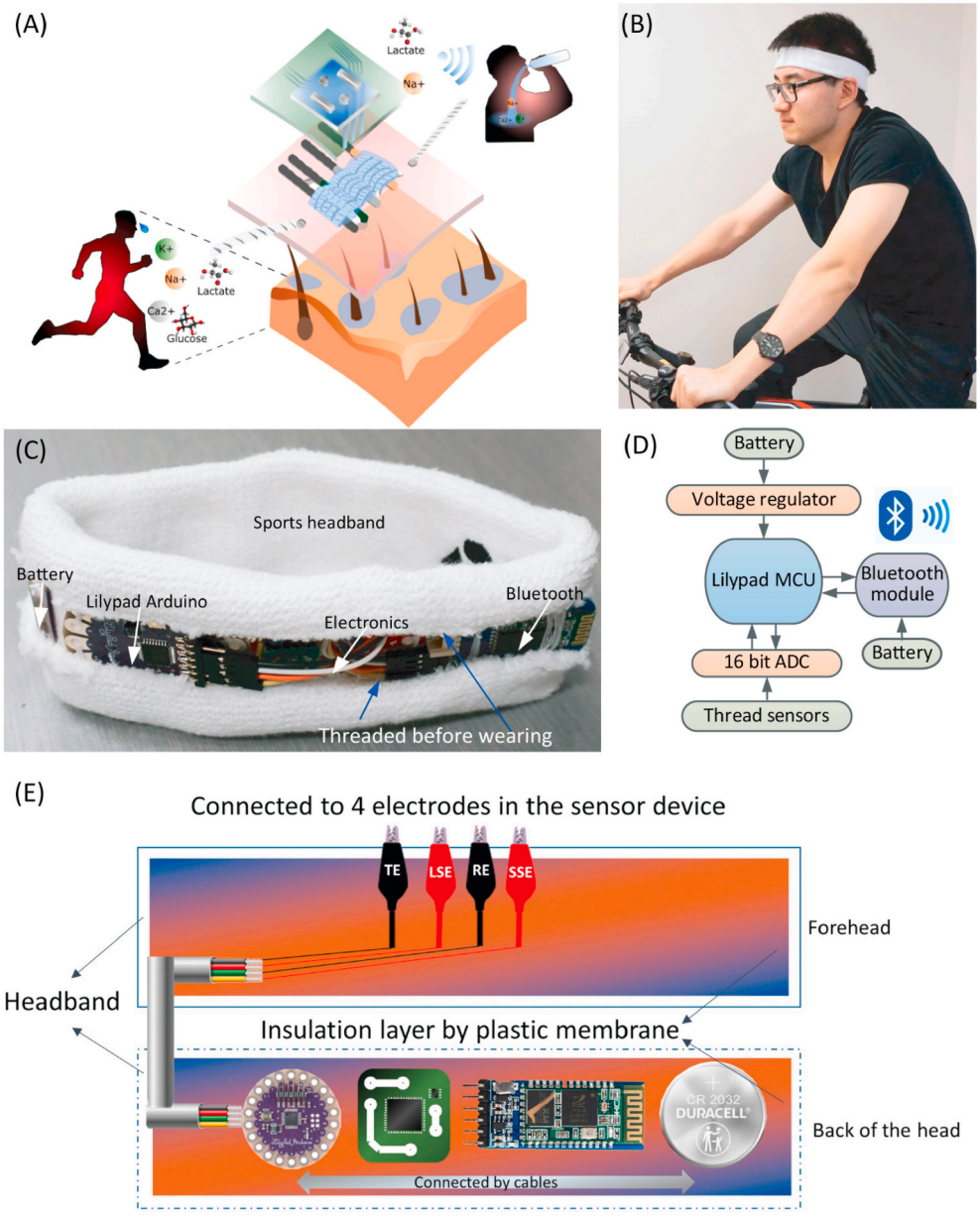

Fig. 1. Design of the wearable biosensor and its 'smart' headband for signal readout. (A) Conceptual scheme of the wearable biosensor for on-body sweat sensing during physical activities. (B) A user wearing the headband. (C) Photograph of the signal readout headband. (D) Schematic architecture of the signal readout circuit. (E) Sectional view of the headband. TE: Trigger electrode (control electrode); LSE: lactate sensing electrode; RE: reference electrode; SSE: sodium sensing electrode.

biosensor, and Fig. 1D shows the architecture of the readout circuit. The circuit includes an Arduino Lily pad, a miniature 16-bit analog-to-digital (A/D) converter (ADS1115, Adafruit), signal processing electronics, a lithium battery (CR2023), and a low-power Bluetooth module (HC-06, Robotshop; for wireless signal transmission). Fig. 1C shows the headband wrapping the circuit before closing. The circuit was pre-calibrated using a DC voltage supplier (E3649A, Agilent) and a digital multimeter (Model 175, Fluke).

For good appearance, the cables, electronics, and battery were placed and hidden in the sweat headband. In order to insulate sweat and prevent it from wetting the electronics, we placed a plastic membrane inside the headband for insulation, which was laid flat and sewn into the band. A schematic diagram (Fig. 1E) shows the built-in design of wires, connectors, and electronics. Note that the smart headband is reusable by the same user. For each measurement, the user only needs to connect a single-use biosensor patch with the same headband and its integrated electronics.

2.3. Thread-based biosensor design

The thread-based biosensor was implemented in the form of an adhesive patch, including a polyester frame, four thread electrodes, a cotton thread wrapping around the four electrodes and thus assembling them with the polyester frame, and double-sided tape to attach the electrochemical cell assembly to human skin. As schematically shown in Fig. 2A, the four thread electrodes are an LSE, an SSE, a RE, and a control electrode, where the LSE and the SSE individually form two electrochemical cells with the RE. The LSE and the SSE were coated with ZnO NWs to improve their surface-area-to-volume ratio and electron transport efficiency (Li et al., 2015). During enzymatic lactate detection, the lactate is oxidized by lactate oxidize immobilized on the LSE, causing free electrons generated and transported between the LSE and the RE and thus an EMF difference produced between the LSE and the RE. In selective sodium ion sensing, the sodium ion exchange between the sample solution and the SSE causes an EMF difference between the SSE

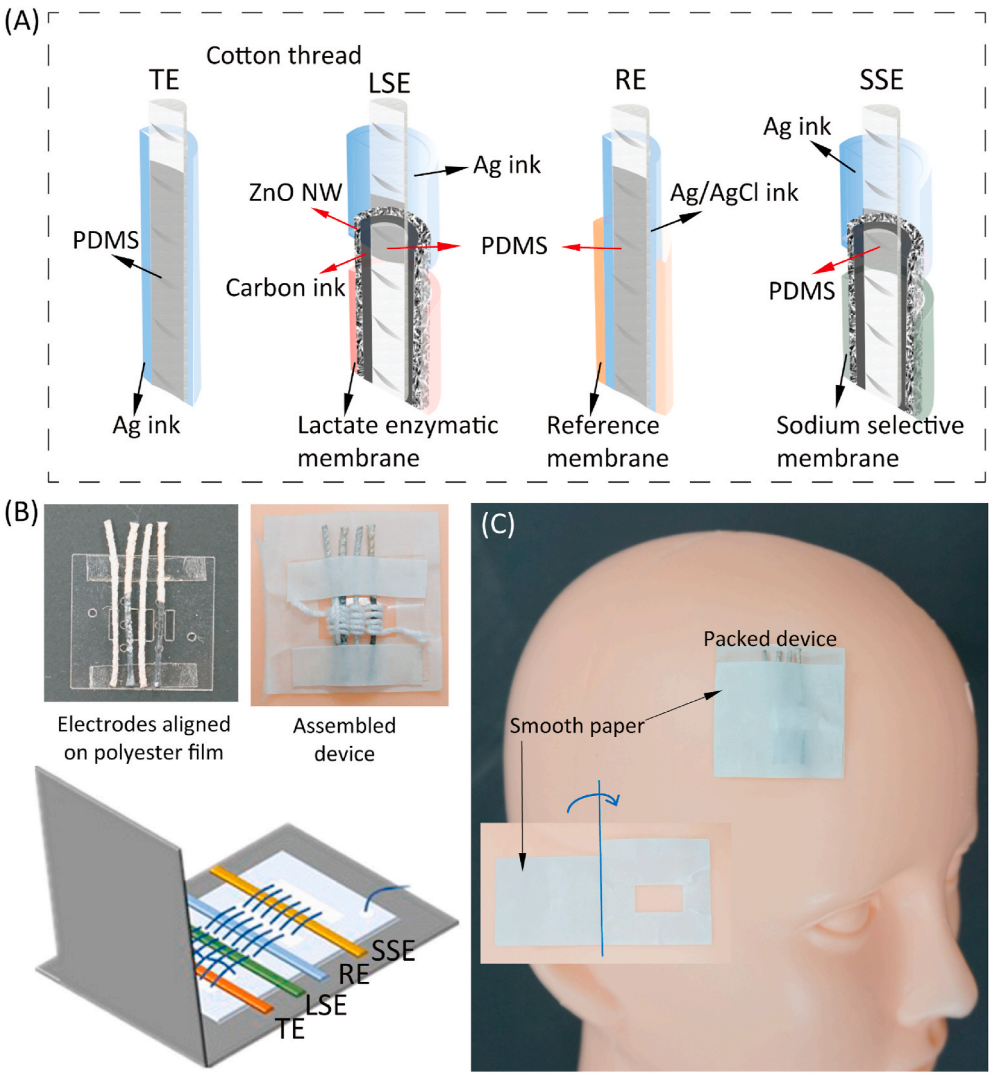

Fig. 2. Biosensor patch design and fabrication. (A) Cross-section view of electrodes showing different material layers. (B) Assembly of the biosensor patch. (C) A biosensor patch attached on a plastic head.

and the RE. The EMF difference quickly stabilizes after the reaction of lactate and lactate enzyme or the sodium ion exchange at the solution-electrode interface reaches its equilibrium, which is used as the biosensor output indicating the lactate or sodium ion concentration. The detailed sensing processes for lactate and sodium ion will be discussed in Section 3.

To fabricate the biosensor patch, a polyester film was laser-cut into the frame shown in Fig. 2B (left), and the four fabricated electrodes were wrapped onto the polyester film using a cotton thread. The CE and the LSE were tightly wrapped together (the left two electrodes in the left photograph of Fig. 2B), and the RE and the SSE wrapped separately onto the polyester frame (the right photograph of Fig. 2B). The cotton thread windings around the LSE and the SSE can absorb sweat fluid and thus serve as reaction reservoirs for lactate and sodium ion detection. After the electrodes were assembled onto the polyester frame, the electrode patch was sandwiched by double-sided adhesive tape with its smooth paper backing facing outside as the protection cover (Fig. 2B). As shown in Fig. 2B and C, we opened a small window (4 mm × 8 mm) on the device to get in contact with the human head skin. In this small window, the cotton thread in the device (Fig. 2B) is in contact with the skin, which could collect sweat. Following the route of the cotton thread, it transfers the sweat from the window to different working areas of the biosensors, and thus saturate the electrodes. A window was laser-cut into the protection cover to expose the thread electrodes to the skin. The patch was then attached on the human forehead where sweat accumulates, with cotton thread in contact with the skin (Fig. 2C). Through experiments, we found that 50 μL of artificial sweat saturated all the cotton thread windings on the patch and was sufficient for the lactate and sodium ion detection.

2.4. Sensing electrode fabrication

To prepare the LSE and the SSE, thread-based carbon electrodes need to be fabricated. A 10 cm cotton thread was first impregnated with uncured PDMS (base-curing agent mixing ratio at 10:1) and baked at 90 °C for 6 h, rendering the thread non-wicking and preventing fluid transport along the thread. Then the thread was coated by carbon ink though roll-printing to cover half of the PDMS portion and 1 cm bare cotton yarn, and hung over a 75 °C hotplate for drying. This roll-printing process was repeated another twice to ensure uniform carbon coating on the thread with even thickness and avoid any cracks on the carbon surface. After drying, the electrodes were washed in deionized (DI) water twice and dried in room temperature before ZnO-NW growth. Fig. 3A shows a scanning electron microscopy (SEM) photograph of the surface of a thread-based bare carbon electrode. Fig. 3B schematically illustrates the cross-sectional view of the thread-based ZnO-NW

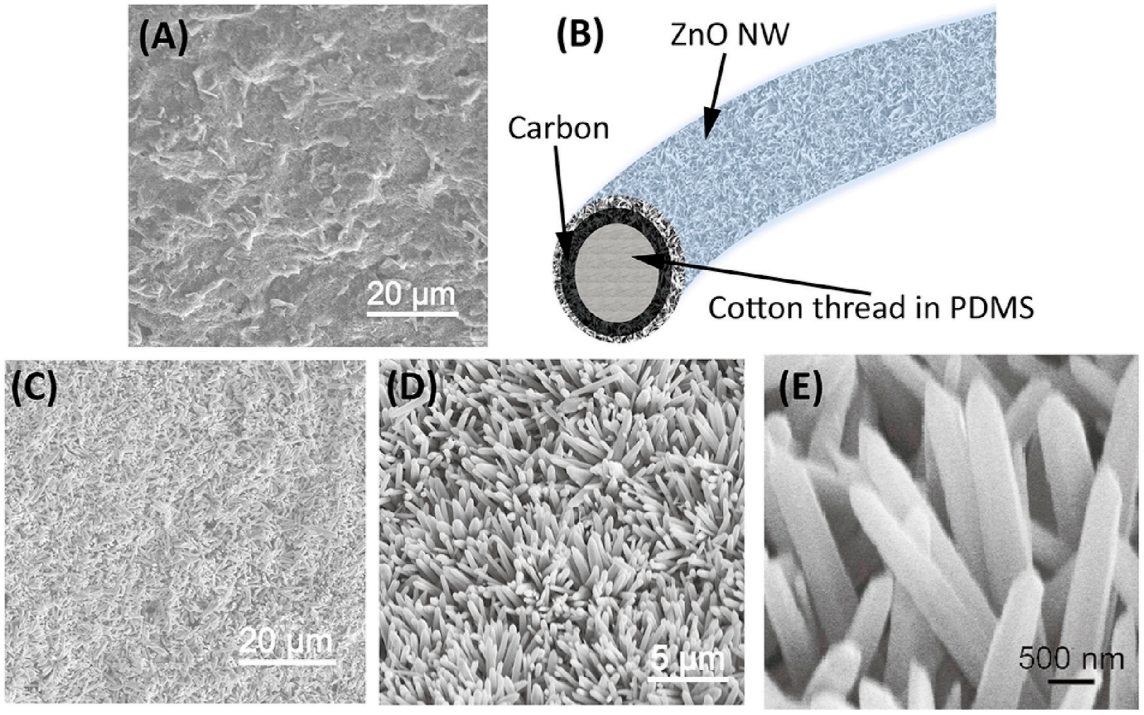

Fig. 3. ZnO-NW growth on carbon electrodes. (A) Bare carbon electrode surface. (B) ZnO-NW electrode surface. (C)(D) and (E) SEM photographs of ZnO-NW electrode at three different magnifications.

electrode.

2.5. ZnO-NW growth on carbon electrodes

The ZnO NWs were grown on the carbon-coated electrodes through a hydrothermal process modified from a previous protocol (Li and Liu, 2016; Li et al., 2015). The hydrothermal synthesis of ZnO NWs relies on the reactions of ZAD, ZNH and HMTA. Through hydrolysis reaction, HMTA generated NH_3 and further provided the hydroxide ions (OH^-) for ZnO NWs growth. ZAD and ZNH provided the Zinc ions (Zn^{2+}) in aqueous solution. The combination of Zn^{2+} and OH^- formed $Zn(OH)_2$, which facilitated the growth of ZnO NWs after dehydration. ZnO nanoparticles (ZnO NPs) were first synthesized in ethanol solution and applied to the working electrode for hydrothermal growth of ZnO NWs. 17.6 mg of ZAD and 5 mg of NaOH were dissolved into two separate flasks each containing 20 mL of pure ethanol and incubated on a 70 °C hotplate with continuous stirring for 20 min. The ZAD solution was then diluted with 20 mL of pure ethanol and then heated at 70 °C with continuous stirring for 30 min. After the ZAD and the NaOH solutions were cooled to room temperature, the NaOH solution was slowly added into the ZAD solution with continuous stirring. The mixture was incubated in a 60 °C oven for 2 h to crystallize the ZnO NPs and form a colloidal seeding solution. Ten entire carbon-coated electrodes were immersed in the seeding solution for 3 min and dried at 86 °C for 3 min, and this immersing/drying process was repeated for three times to achieve uniform ZnO-NP coating on the WEs.

A mixture of ZNH and HMTA was made to grow ZnO NWs on the ZnO-NP-seeded electrodes. 2.98 g of ZNH and 0.7 g of HMTA were separately dissolved into two 500 mL flasks each filled with 190 mL of DI water, forming ZNH and HMTA concentrations of 50 mM and 25 mM, respectively. The two solutions were mixed after thorough dissolution. 10 mL of AH was then added to the mixture solution to obtain the final growth solution, and the AH in the growth solution ensures high growth efficiency of the ZnO NWs by suppressing the homogeneous nucleation (Li et al., 2015). The final mixture was preheated in an oven at 86 °C for 15 min, and 10 ZnO-NP-seeded electrodes were then placed into the growth solution at 86 °C for growth of 8 h. After the growth was completed, the ZnO-NW-coated electrodes were washed in DI water and dried under ambient environment. Fig. 3C–E shows the morphology of the ZnO NWs on an electrode under SEM at different magnifications. The thread cotton microfibers were uniformly covered with ZnO NWs standing radially outward, with average NW width and density of 392 ± 51 nm (n = 5) and $2.80 \pm 0.21/\mu m^2$ (n = 5), respectively. After the ZnO-NW growth, Ag ink was applied to the bare cotton thread end of the WE through roll printing, which electrically connected the carbon ink layer for electrical connection. After this step, the ZnO-NW-coated electrode was ready for coating of the lactate and sodium sensing membranes. Note that the ZnO-NW growth on the carbon electrode made the electrode surface slightly grayish, as shown in Fig. 2B.

2.6. Fabrication of the reference and control electrodes

As each electrochemical cell only contains two electrodes, the shared RE also acts as a counter electrode (CE) and ensures a complete path of electron transfer through each cell. To fabricate the RE, a 4 cm thread was completely impregnated with PDMS and cured at 90 °C for 6 h. Then, Ag/AgCl ink was rolling-printed to the thread and dried at 75 °C for 5 h. A PVB membrane solution was prepared by dissolving 78.10 mg PVB and 50 mg NaCl in 1 mL methanol according to a previously reported recipe (Bandodkar et al., 2014). It contains electrolytes and can form a nanoporous structure that allows the exchange of electrolytes with the solution, providing a stable potential insensitive to changes in the ion concentration over a wide concentration range (Bandodkar et al., 2014). 5 μL of PVB membrane solution was applied to the Ag/AgCl electrode twice and then dried to form the ultimate RE.

A control electrode was designed to indicate the state of sweat absorption on the biosensor, which is based on the resistance between the sensing electrode and the control electrode. To generate the control electrode, 4 cm thread was coated with PDMS to prevent interference potential change caused by the liquid leakage. Ag ink was rolling-printed to the thread and dried at 75 °C for 5 h. Then, the electrode is ready to use.

2.7. Preparation of sensing membranes on the sensing electrode

To fabricate the LSE, a ZnO-NW-coated electrode was functionalized with the lactate enzymatic membrane. Firstly, a paired Nafion-TTF^+ reactive membrane was formed by applying 3 μL of 0.5% v/v Nafion and 5 μL of 0.1M TTF ethanol/acetone [9:1 (v/v)] solution to the electrode. The coating of Nafion-TTF membrane was repeated to secure the uniform coating on the thread electrode. Then, 3 μL of LO_x solution (200 unit/mL) was coated on the electrode and dried under ambient condition; this surface was later coated with 3 μL of 1 wt % chitosan solution prepared in 1 wt % acetic acid (heavily stirred for 24 h). The electrode was finally cross-linked with 15% v/w glutaraldehyde (GA) vapor in a sealed chamber and maintained at 4 °C for overnight. Before reacting with lactic acid, the electrode was pre-scanned using cyclic voltammetry (CV) from −0.25 V to 0.4 V twice to form TTF^+ as the mediator for lactate enzymatic reaction (Liu and Deng, 1995; Palleschi and Turner, 1990).

For SSE fabrication, a ZnO-NW-coated electrode was coated with 5 μL of sodium-selective membrane solution twice. This membrane solution consisted of 1 mg sodium ionophore X, 0.55 mg Na-TFPB, 33 mg PVC, and 65.45 mg DOS dissolved in 660 mL of nitrogen-purged THF with thorough mixing, according to a previous recipe (Bandodkar et al., 2014). The electrode was dried in the ambient environment after the membrane coating.

3. Results

3.1. Sensing electrode characterization in bulk solution

To confirm the feasibility of the biosensor design, we conducted trial-and-error tests of the LSE and SSE in bulk solutions of artificial sweat. For calibration of lactate detection, the artificial sweat is supposed to contain no lactic acid. Thus, we removed the lactic acid component from the artificial sweat by preparing it to be 20 g/L NaCl, 17.50 g/L NH_4Cl, 5 g/L acetic acid with the pH adjusted to 7.0 using NH_4OH. For calibration of sodium detection, the artificial sweat should contain no sodium. Thus, we removed the sodium component was removed from the artificial sweat by preparing it to be 35.80 g/L NH_4Cl, 5 g/L acetic acid and 15 g/L lactic acid with the pH adjusted to 7.0 using NH_4OH.

3.1.1. LSE characterization in bulk solution

Before characterizing the biosensor, the LSE electrode, sequentially coated with Nafion, TTF, LO_x, chitosan, and GA, was pre-conditioned through cyclic voltammetry to form the Nafion-TTF^+ pair for electrochemical detection of lactate. An LSE and a RE were put into a 1.5 mL tube filled with 1 phosphate-buffered saline (PBS) for CV scanning. During the CV scan, the TTF was oxidized to TTF^+ and the Nafion-TTF^+ pair was formed. Equation (1) illustrates the reaction mechanism forming the Nafion-TTF^+ pair. When the positive potential reached a certain level, the TTF was oxidized to TTF^+; simultaneously, the Na^+ ions in the sulphonate group of Nafion were substituted with TFF^+, and the Na^+ ions were released to the phosphate buffer (Liu and Deng, 1995). Fig. 4A shows two cyclic voltammograms measured during twice of CV scanning between −0.25 V and 0.45 V at a scan rate of 20 mV/s. The high level of overlap between the two cycles indicates the repeatability and reversibility of the generated TTF^+ as a surface-bound species. TTF^+ was then used as the mediator for enzymatic detection of lactate.

$$TTF + SO_3/Na^+ \rightarrow SO_3/TTF^+ + Na^+ + e^- \quad (1)$$

After the LSE pre-conditioning, we performed lactate detection using the LSE and the RE in spiked bulk solutions. We used two artificial sweat solutions at lactate concentrations of 0 mM and 25 mM. 1.5 mL of sweat solution was filled in a 1.5 mL tube, and the LSE and the RE were put into the solution with only the sensing part of the LSE immersed into the solution and the conductive part outside. Fig. 4B shows data plots of the LSE/RE potential difference measured from the solutions with zero and 25 mM lactic acid. With zero-concentration lactic acid, the measured potential reached ~65 mV at 20 s. With 25 mM lactic acid, the potential difference reached ~98 mV at 20 s, showing that the LSE properly responded to the presence of lactate in the solution. During the reaction, lactate diffused from the solution into the enzyme membrane and got oxidized by the lactate oxidase; simultaneously, the TTF^+ was reduced to TTF, as illustrated by equation (2). The change in the concentration ratio of TTF^+ to TTF in the enzyme membrane can be detected through the EMF between the LSE and the RE. The potential difference with and without lactate indicated that TTF^+ in the Nafion membrane could act as an electron-transfer relay system between the centers of lactate oxidase and the ZnO-NW-coated LSE.

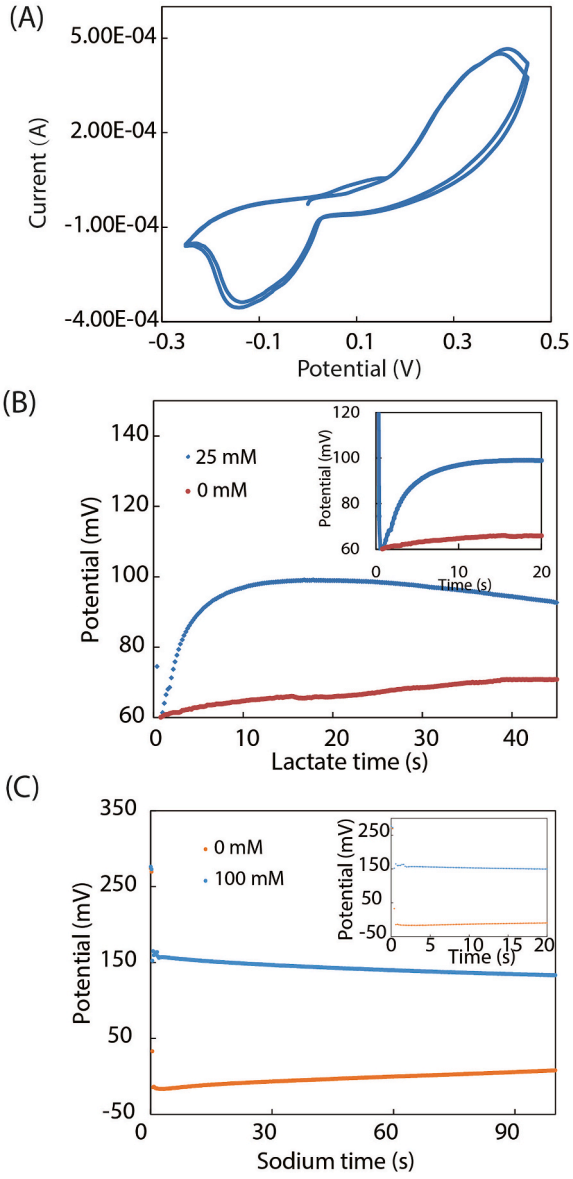

Fig. 4. Sensing electrode characterization in bulk solutions. (A) Cyclic voltammograms of the lactate-sensing electrode. (B) Measured LSE/RE potential difference versus time for lactate detection at 0 mM and 25 mM. (C) Measured SSE/RE potential difference versus time for sodium detection at 0 mM and 100 mM.

$$Lactate + 2TTF^+ \rightarrow pyruvate + 2TTF + 2H^+ \quad (2)$$

3.1.2. SSE characterization in bulk solution

The SSE was coated with a sodium ion-selective membrane of DOS/PVC/Na-TFPB based on the sodium ionophore X. DOS was used as the plasticizer to provide a homogeneous organic phase of the membrane, reduce its viscosity, and ensure relatively high mobility of the membrane constituents (Mihali and Vaum, 2012). It also maintained the ion-exchange characteristic of the membrane and ensures the ion selectivity caused by its polarity and dielectric properties (Mihali and Vaum, 2012). The polymeric matrix of PVC provided mechanical stability of the membrane, and its inertial characteristic prevented other chemical interactions with the target ions. Na-TFPB was used as a lipophilic cation exchanger to ensure the cation selectivity. The sodium ionophore X acted as an ion carrier and formed relatively strong, selective, and reversible complexes with the target ions, and thus prevented the ion-exchange of any interfering ions. This structure of sodium ion-selective membrane has a superior influence on the selectivity of potentiometric sodium ion measurements.

No pre-conditioning was required for sodium detection. We tested the SSE in bulk artificial sweat solutions with 0 mM and 100 mM sodium ions. 1.5 mL of the sample solution was filled in a 1.5 mL tube, and an SSE and a RE were then put into the tube with only the sensing part of the SSE immersed into the solution and the conductive part outside. Redox processes did not occur at the SSE. Instead, the sodium ion partitioned into the organic membrane with the help of ionophore. During the continuous ion-exchange process, an equilibrium was established at the solution-membrane interface, and the charge separation across the interface caused a phase-boundary potential difference across the membrane that can be measured between the SSE and the RE. Fig. 4C shows the SSE/RE potential difference plots measured from the solutions with 0 mM and 100 mM sodium. An obvious potential difference was observed from ~0 mV for 0 mM and ~ 130 mV for 100 mM at 100 s, which proves the feasibility of using this mechanism for sodium sensing.

3.2. Biosensor calibration

After confirming the sensing mechanisms, we calibrated the assembled biosensor for lactate and sodium detection. The biosensor patch was first assembled according to Fig. 2B. Then, 50 μL of spiked sweat solution was pipetted to the cotton thread wrapping all electrodes to completely wet the electrodes. At the same time, the smart headband was triggered to read the data from the biosensor. Fig. 5A shows the raw potential difference curves measured at different lactate concentrations of 0–25 mM. The signal at 20 s post triggering was measured as the final readout. Fig. 5B shows the calibration plot of the biosensor for lactate detection (n = 6 samples). A relatively fast time point was preferred for data reading during both off-body and on-body monitoring. In our preliminary experiments, we compared the results of multiple tests. At 20 s, the data had been largely stabilized, which is a relatively fast and stable time point. We also found the measurement at 20 s give us reproducible results.

One can see that the measured potential difference increases from ~70 mV at 0 mM lactate to ~92 mV at 25 mM lactate. Fig. 5C shows the raw potential difference curves measured at different sodium concentrations of 0–100 mM. The final readout signal was also measured from the raw curves at 20 s post triggering. Fig. 5D shows the calibration plot of the biosensor for sodium detection (n = 6 samples). In Figs. 4B and 5A, we found a non-zero potential difference at zero lactate concentration. This potential difference may be caused by the original charge difference between the electrodes. The same phenomenon was observed between sodium sensing electrode and reference electrode (Figs. 4C and 5B), and also in previous reports (Gao et al., 2016; Wang et al., 2020). After comparing the potential differences between the target and the zero lactate, we could differentiate and calculate the target concentration.

The LOD was calculated from the calibration plot as the lactate/

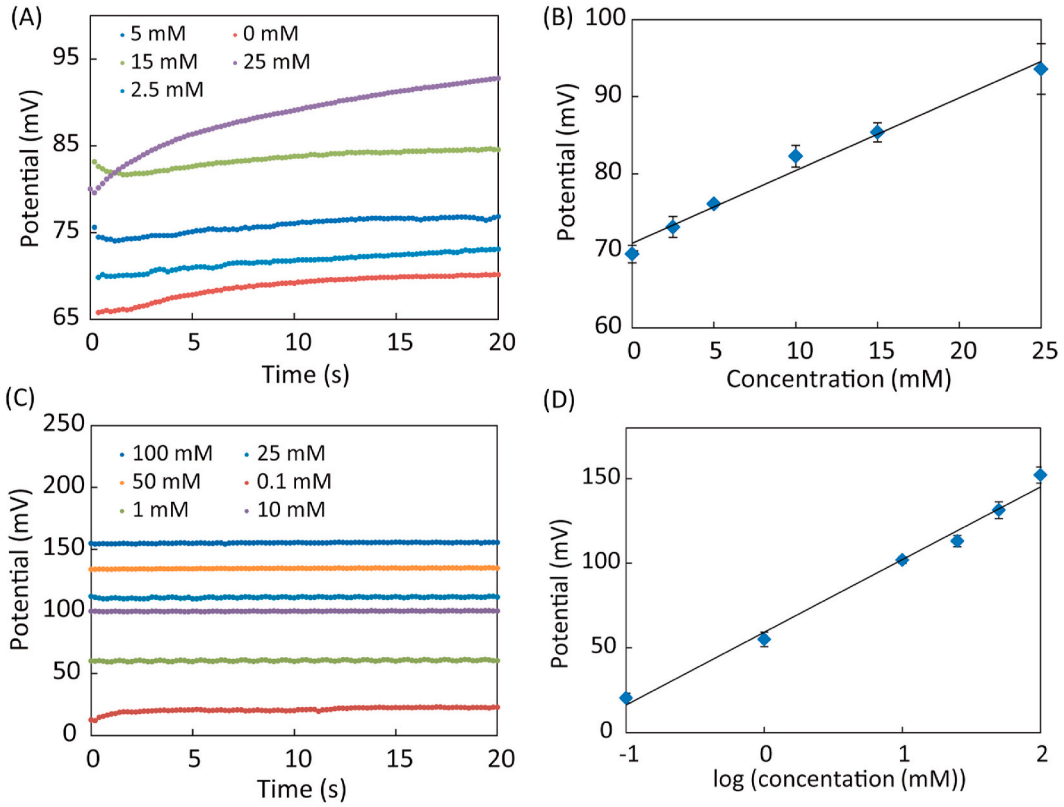

Fig. 5. Biosensor calibration results. (A) Raw potential difference curves measured from solutions at different lactate concentrations. (B) Calibration curve for lactate detection (n = 6 samples). Linear regression equation: y = 0.94x + 71 (R^2 = 0.9831). (C) Raw potential different curves measured from solutions at different sodium concentrations. (D) Calibration curve for sodium detection (n = 6 samples). Linear regression equation: y = 42.9x+59.2 (R^2 = 0.9897).

sodium concentration corresponding to the zero-concentration output signal plus three times the standard deviation of the zero-concentration output data. The LODs of the biosensor for lactate and sodium detection are 3.61 mM and 0.16 mM, respectively. The linear ranges (0–25 mM for lactate and 0–100 mM for sodium) of both lactate and sodium calibration plots fully cover the clinically relevant ranges of lactate (9–25 mM) (Jia et al., 2013) and sodium (0–100 mM) in sweat (Bandodkar et al., 2014).

3.3. Off-body testing using real human sweat

To further test the performance of the biosensor for real human sweat testing, we recruited a healthy male volunteer to participate in the off- and on-body testing of the biosensor. At the time of testing, the volunteer was 28 years old and had no prior history of heart diseases, diabetes, or skeletomuscular pain. The study protocol was approved by the Research Ethics Board (REB) of the University of Toronto (protocol #35992; approval date: July 31, 2018), and evaluated to have low group vulnerability and low research risk. Before the studies, a consent form was signed by the volunteer, with all test procedures and possible risks notified. Both the off- and on-body tests were performed in strict compliance with the REB-approved protocol.

We first performed off-body testing of the biosensor using real human sweat collected from the volunteer after 30 min of exercise. Our biosensor tested the lactate and sodium levels in the volunteer's sweat to be 13.16 ± 0.83 mM (n = 6 tests) and 92.9 ± 5.00 mM (n = 6 tests), respectively. The clinically relevant ranges are 9–25 mM for sweat lactate (Jia et al., 2013) and 0–100 mM for sweat sodium (Bandodkar et al., 2014). Concentrations beyond this range may be related with diseases such as lactic acidosis and pancreatic cystic fibrosis. The volunteer we recruited had no prior diseases. The data 13.16 ± 0.83 mM (lactate) and 92.90 ± 5.00 mM (sodium) obtained from his sweat were within the clinically relevant range.

We also performed standard lactate and sodium tests of the same sweat sample using an enzyme-based colorimetric lactate assay and a commercial sodium selective ion electrode (# EW-27504-30, Cole-Parmer), respectively. Both values were in good agreement with the standard test results of 13.26 ± 0.57 mM (n = 6 tests) for lactate and 89.90 ± 2.42 mM (n = 6 tests) for sodium. Fig. 6A compares the off-body testing results from the biosensor and the standard tests, which shows no obvious difference between the biosensor results and the standard results. Fig. S1 show the calibration results using an enzyme-based colorimetric lactate assay (Li and Liu, 2014) on a paper-based 96-well plate. Fig. S2 shows the calibration results of sodium ion using the commercial sodium selective ion electrode.

Before on-body testing, experiments were conducted on a plastic head model (Fig. 2B) to mimic the real working condition of the biosensor on the human skin of a person during exercise. We firstly connected the biosensor patch to the smart headband, started the vibration/movement and initiate the data measurement. Then, we attached the biosensor patch to the forehead of the plastic head model (Fig. 2B) with the protection cover opened. 50 μL of artificial sweat with

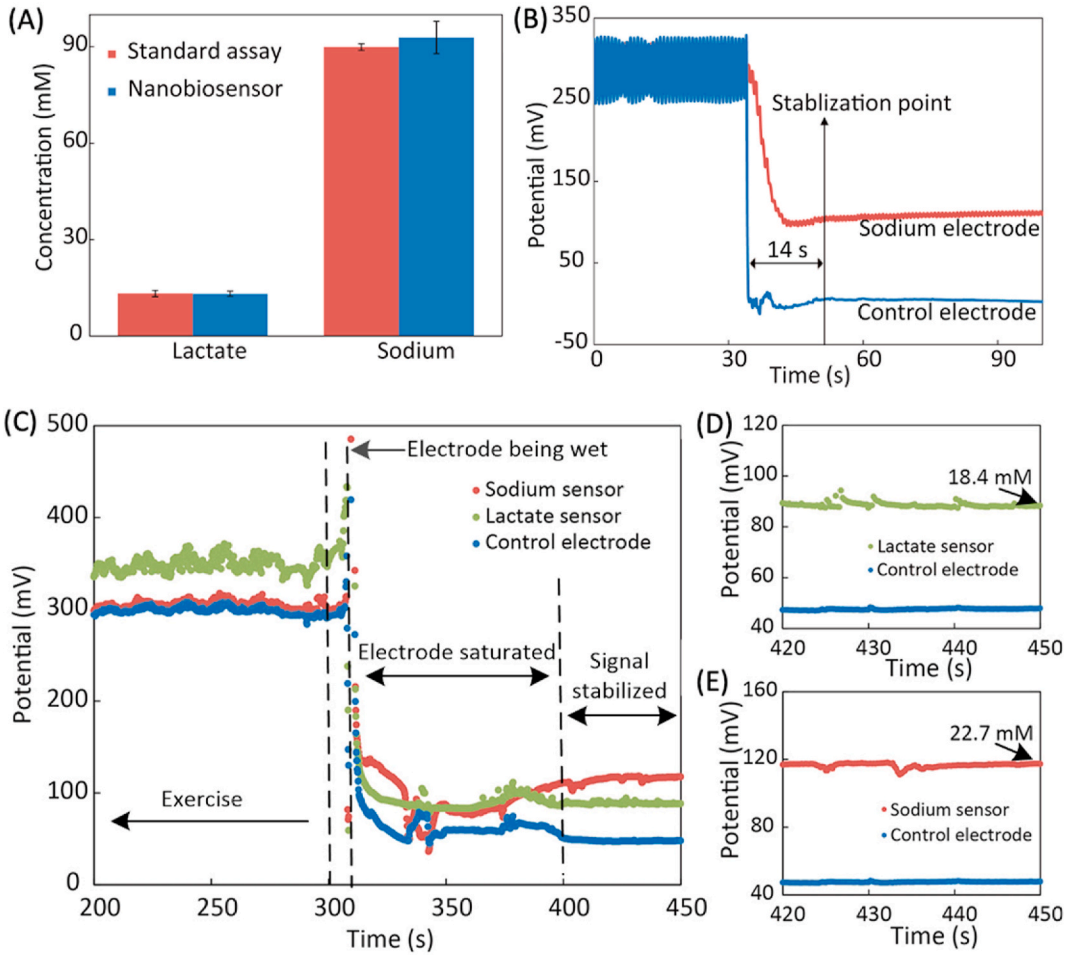

Fig. 6. Off- and on-body testing of the biosensor using real human sweat sample. (A) Comparison of the off-body lactate and sodium testing results from the biosensor and the standard test on human sweat (n = 6 tests). (B) Pseudo-on-body sweat testing showing the stabilization point determined by the control electrode. (C) on-body measurement curves since the start of the user exercise. (D) lactate concentration determination after stabilization. (E) sodium concentration determination after stabilization.

50 mM sodium was added for off-body testing. In our preliminary experiments, we found that there was a critical volume to fully saturate the cotton and the four electrodes. Otherwise, the sensor signals were unstable and inaccurate. With the 50 μL of artificial sweat, the sensor signals reached their steady states in relatively short time. With more than 50 μL of artificial sweat, the potential difference did not reveal a big difference as the cotton thread has been fully saturated. In our experiments, we also found that the typical sweat volume secreted from a 4 mm x 8 mm skin area of the volunteer we recruited during exercise in 30 min is much higher that 50 μL, which was evidenced by the quick signal stabilization shown in Fig. 6C.

During the measurement, the headband was worn on the plastic head. Fig. 6B shows the output signal of LSE/RE potential difference and the control electrode signal (potential difference between the control electrode and the RE) on the head model. With the addition of artificial sweat from the pipette, the potential difference between the control electrode and the RE rapidly dropped to a low potential at ~0 mV within ~14 s. The drop of the potential difference was caused by the penetration of the sweat solution into the cotton thread wrapping all the electrodes and thus the complete wetting of the electrodes. At this time point (~14 s after sweat injection), the potential difference measured from the SSE also reached to a stable level, showing that the control electrode and the sensing electrode simultaneously responded to sweat penetration to the biosensor without obvious delay. The plastic head was moved and vibrated during the entire testing process (0–100 s in Fig. 6B). Upon sweat application, no obvious shifting of the potential difference values measured from the SSE and the control electrode was observed under these situations, showing the mechanical and electrical reliability of our wearable biosensor platform. With our current biosensor patch design, the bending of the biosensor patch upon attaching to the skin is negligible as the patch size (2 cm × 2 cm) is relatively small and the patch is placed on the flat forehead skin. With firm electrical connections between the biosensor electrodes and the signal readout, our entire biosensor platform showed faithful responses to sweat lactate and sodium with low noise levels during head movement and vibration. With its mechanical and electrical reliability confirmed, the wearable biosensor and its smart headband were carried forward to on-body testing on the recruited volunteer.

3.4. On-body testing during user exercise

The on-body testing was conducted on the same male volunteer after the off-body human sweat test. In the headband, four conductive wires came out of the microprocessor, and four clips were connected to the ends. The four clips were hidden in the headband and wrapped with insulating tape for isolation. During detection, the four clips will be connected to the silver parts of the electrodes in the patch device (Fig. 2B). Through that, signal transmission could be successfully achieved. To collect data of on-body testing, we use the Arduino Lilypad microprocessor with Bluetooth and data processing electronics (Fig. 2). Before data collection, we matched the headband Bluetooth with the Bluetooth from the personal computer (MacBook Air). On the computer, we opened the Arduino software serial data receiving interface to receive data. We wrote codes in the Arduino software to realize the functions of data processing and data receiving. After the acquisition was complete, we manually stored the data in TXT format for subsequent analysis.

Through the off-body testing of the volunteer sweat, we found that his sweat sodium concentration of 89.90 ± 2.42 mM is much higher than the normal sweat sodium level (15–65 mM) of a healthy person (Rosner and Kirven, 2007). Through a post-testing survey, we found that the volunteer has the habit of consuming salty diets with high sodium. Thus, we asked the volunteer to have one-week of low-sodium diet intake before carrying out the on-body test. For the on-body test, the volunteer attached the biosensor patch onto the skin of his forehead and wore the headband with its electronics connected to the biosensor electrodes. With the sweat testing initiated, the volunteer had a 5-mins intense exercise of staircase climbing and a 15-min rest. Fig. 6C shows the raw output signals measured on the LSE, the SSE, and the control electrode during the 5-mins exercise and the first 2.5 min of rest. One can see that, during the user movement (0–300 s in Fig. 6C), the three potential difference values remained relatively stable (in the range of 290–365 mV) with certain noises, indicating the open circuit between the LSE/SSE/-control electrode and the RE. During the exercise, the perspiration from the user skin was gradually absorbed by the cotton thread (that wrapped the electrodes) of the biosensor, and started to wet the electrodes at ~310 s (10 s after the 5-min exercise).

In Fig. 6C, the significant change of the potential signal is not due to the ion detection process itself, but rather due to the saturation process of the electrode by the sweat. After that, it only took another 20 s to stabilize between 400 s and 420 s. Between 420 s and 450 s, the results were largely stabilized, which was ready for lactate and sodium signal measurement. Correspondingly, the three potential difference curves measured from the LSE, the SSE, and the control electrode rapidly decreased to a much lower level of 35–105 mV and finally stabilized between 420 s and 450 s. The stable LSE and SSE signals at 450 s (Fig. 6D and E) were used to determine the lactate and sodium concentrations in the user sweat. The lactate and sodium concentrations were determined to be 18.4 mM and 22.7 mM, respectively. It can be observed that after one-week diet control, the volunteer's sweat sodium level dropped into the normal range of sweat sodium concentration of a healthy person.

3.5. Analytical performance comparison

Current textile-based biosensors usually employ single detection mechanism, such as enzymatic assay (Luo et al., 2018; Promphet et al., 2019) or ion-selective assay (Coppedè et al., 2020; Wang et al., 2020). Tables 1 and 2 summarize the analytical performance between our work and other similar wearable textile-based biosensors for lactate and sodium detection, respectively. For the measurement of sodium (Table 2), our biosensor achieved similar LOD and linear ranges compared with previous studies (Coppedè et al., 2020; Wang et al., 2020). Note that we have demonstrated simultaneous detection of enzymatic and ion selective assays on cotton threads for both off-body and on-body measurements, indicating the reliability and versatility of our wearable biosensor.

The textile biosensors based on enzymatic assay and amperometry provide better LOD (Luo et al., 2018; Wang et al., 2021) than ours (Table 1). However, for on-body measurement, it is beneficial to adopt a detection method that is sufficiently accurate and requires a simple and reliable signal readout circuit; this makes the wearable biosensor more practical for real-world applications. The detection principle we employed was potentiometry. Compared with colorimetry (Promphet et al., 2019), it is not sensitive to the ambient illumination, making it easier to have quantitative and accurate analysis. In contrast to amperometry (Luo et al., 2018; Wang et al., 2021), the potentiometric method does not rely on external electrical triggering, and thus only

Table 1
Analytical performance comparison of our work and other similar wearable textile-based biosensors for lactate detection.

Performance	Lactate (our work)	Luo et al. (2018)	Promphet et al. (2019)	Wang et al. (2021)
LOD	3.61 mM	258.2 μM	N/A	0.14 mM
Linear range	0–25 mM	476.20 μM–3.13 mM	0–10 mM 12.5–25 mM	0–5 mM 10–30 mM
Detection method	Enzymatic and potentiometric	Enzymatic and amperometric	Enzymatic and colorimetric	Enzymatic and amperometric
Functional materials	ZnO NWs	CNT	Chitosan	Au NWs
Textile	Headband	Glove	Cotton	T-shirt

Table 2
Analytical performance comparison of our work and other similar wearable textile-based biosensors for sodium detection.

Performance	Sodium (our work)	Wang et al. (2020)	Coppedè et al. (2020)
LOD	0.16 mM	N/A	0.10 mM
Linear range	0.1–100 mM	0.1–100 mM	0.1 mM-1 M
Detection method	Ion-selective membrane and potentiometric	Ion-selective membrane and potentiometric	Ion-selective membrane and potentiometric
Functional materials	ZnO NWs	AuNP/CNT	Conductive polymer
Textile	Headband	Armband	Acrylic textile thread

requires a voltage measurement circuit for signal readout. This makes the integration of the readout circuit and wearable biosensor patch easier and more reliable. In the future, the target analyte of our biosensor could be easily extended other types of metabolic marker in sweat, and the overall biosensor patch design and the signal readout circuit will remain the same. The millivolt-level EMF output also ensures safe and user-friendly operation of the wearable biosensor platform.

4. Discussion

In recent years, wearable sensors for biochemical sweat analysis have attracted tremendous interest from both academia (Bandodkar et al., 2019; He et al., 2019; Zhai et al., 2020) and industry (Brothers et al., 2019; Ferreira et al., 2019; Seshadri et al., 2019). Efforts have been spent on the design and development of miniaturized non-invasive measurement platforms capable of real-time on-body sweat collection and analysis (Brothers et al., 2019; Min et al., 2020). In this study, we developed a thread-based wearable sweat nanobiosensor, which integrates thread-based electrodes decorated with semiconductor ZnO NWs, for simultaneous detection of lactate and sodium in human sweat during perspiration. The biosensing principles were based on enzymatic oxidation of lactate and selective exchange of sodium ions, both occurring on their sensing electrodes, and the final readout signals from both reactions are the EMF (potential difference) between the corresponding sensing electrode and the RE.

An integrated smart headband was developed to electrically interface with the wearable biosensor, quantify the readout signals from the biosensor during on-body measurement, and transmit the measurement data to an external receiver such as a computer or a smartphone. We experimentally demonstrated the detection of lactate and sodium with linear ranges of 0–25 mM and 0.1–100 mM and LODs of 3.61 mM and 0.16 mM, respectively, covering the clinically relevant ranges of lactate and sodium in human sweat. We also performed real human sweat testing of the biosensor and obtained accurate results that were benchmarked by the standard tests. Using the nanobiosensor, lactate and sodium measurements were conducted on a human volunteer during exercise with robust signal readouts and accurate testing results.

Sweat includes various ions which may interfere with the ZnO nanowires. Our wearable sensors are designed for one-time use, with an estimated manufacturing cost of less than CAD $0.5. We only used it for less than 30 min. Thus, in our experiments we did not test the sensor performance stability over long-term use. Within the 30-min period of testing, the device output varies in an acceptable range, which were reflected by standard deviations in the results (<8%).

In our experiments, we found that the carbon layer on top of PDMS or bare cotton is quite easy to get cracked, which significantly affected the resistance of the electrode. After many repeated experiments, we noticed that the variable resistance of the carbon ink coating had the most significant impact on the stability, repeatability and accuracy of the results. When we coated the surface with much thicker carbon ink, the cracking of the carbon layer was reduced. With little crack, the resistance of the carbon electrode stabilized at about 20 Ω. Therefore, we always performed three thick coatings each time for the carbon electrode on top of the PDMS or bare cotton.

The working principle of our biosensor is based on potentiometry, which relies on the potential difference (EMF) between two electrodes. Although generally less sensitive to amperometric methods, potentiometry provides sufficient sensitivity and requires much simpler signal readout electronics. Thus, it could be low-cost and more accessible than the amperometric methods. In addition, different target analytes need different voltage levels for the amperometric reaction, while the potentiometric method only needs to measure a potential difference from the biosensor. This also simplifies measurement protocols for different analytes.

The lactate and sodium sensing principles we used are lactase-based enzymatic detection and sodium ion selective membrane detection, respectively. These methods are mature and have been demonstrated with good specificity in previous studies (Pirovano et al., 2020; Rathee et al., 2016). Therefore, we did not carry out the specificity and selectivity experiments separately. However, the interfering effect of coexisting substance in our testing samples, like urea, potassium, ammonium, chloride and glucose, could, to some extent, testify the selectivity of the two sensing electrodes. In the future, we plan to use different interfering metabolites in sweat for specificity and selectivity testing.

Our goal was to measure the concentrations of lactate and sodium in sweat in a relatively short time. Therefore, we did not perform experiments on real-time detection of the target analyte and analyze the biosensor's real-time response characteristics. When we conducted off-body calibration, we tried to increase the concentration of the analyst in a stepwise manner to confirm whether the electrode was sensitive to the target. We found that, upon the stepwise change in the analyte concentration, the biosensor output rose slowly. We did not perform quantitative analysis on the signal increase profile. In our future work, we will conduct a systematic analysis on the real-time response of our biosensor and thus reveal the device's dynamic characteristics.

In this study, we have analyzed the off-body real samples through standard methods of colorimetric assay for lactate and commercial selective ion electrode for sodium. We have compared the results between our wearable biosensor and the standard methods (Fig. 6A). For the same sample, we repeated 6 times of measurement using our sensors. The standard deviation is <8%, showing good reproducibility of our biosensor. As the biosensor accuracy and reproducibility has been proved by using the off-body sample, for on-body testing we did not compare the results with these of standard methods. The simultaneous on-body sample collection and testing using both standard assays and our device during exercising are technically challenging. Admittedly, the comparison of our sensors with the standard methods for on-body real samples could further demonstrate the performance of our device. Thus, in our future work we will perform the comparison experiments through recruitment of multiple volunteers. The continuous monitoring by our biosensor will be examined during long-term wearing and exercising by these users. A cellphone application will be created to interface with the smart headband for wireless data transmission and analysis.

5. Conclusions

We developed a fully integrated wearable sweat testing platform based on a thread-based biosensor integrating ZnO-NW-decorated sensing electrodes, for accurate lactate and sodium detection in human perspiration during exercise. Real-time on-body sweat collection and analysis were performed on a volunteer during intense exercise, confirming the accuracy and stability of biosensor in real use. This wearable and low-cost biosensing platform could find practical applications in physiological condition monitoring of human users during fitness.

CRediT authorship contribution statement

Chen Zhao: Conceptualization, Methodology, Investigation, Visualization, Writing – original draft, Writing – review & editing. **Xiao Li:** Conceptualization, Methodology, Investigation. **Qiyang Wu:** Investigation. **Xinyu Liu:** Conceptualization, Methodology, Writing – review & editing, Supervision, Funding acquisition.

Declaration of competing interest

The authors declare that they have no known competing financial interests or personal relationships that could have appeared to influence the work reported in this paper.

Acknowledgments

This work was supported by the Natural Sciences and Engineering Research Council of Canada (RGPIN-2017-06374 and RGPAS-2017-507980), the Canada Foundation for Innovation (JELF-37812) and the University of Toronto (through a Percy Edward Hart Professorship to Xinyu Liu). Qiyang Wu also acknowledges the support from the Chinese Scholarship Council.

Appendix A. Supplementary data

Supplementary data to this article can be found online at https://doi.org/10.1016/j.bios.2021.113270.

References

Alizadeh, A., Burns, A., Lenigk, R., Gettings, R., Ashe, J., Porter, A., McCaul, M., Barrett, R., Diamond, D., White, P., 2018. A wearable patch for continuous monitoring of sweat electrolytes during exertion. Lab Chip 18 (17), 2632–2641.

Anderson, C.M., Freeman, M., Allan, J., Hubbard, L., 1962. Observations on (i) sweat sodium levels in relation to chronic respiratory disease in adults and (ii) the incidence of respiratory and other disease in parents and siblings of patients with fibrocystic disease of the pancreas. Med. J. Aust. 49, 965–969.

Bandodkar, A.J., Jeang, W.J., Ghaffari, R., Rogers, J.A., 2019. Wearable sensors for biochemical sweat analysis. Annu. Rev. Anal. Chem. 12, 1–22.

Bandodkar, A.J., Molinnus, D., Mirza, O., Guinovart, T., Windmiller, J.R., Valdés-Ramírez, G., Andrade, F.J., Schöning, M.J., Wang, J., 2014. Epidermal tattoo potentiometric sodium sensors with wireless signal transduction for continuous non-invasive sweat monitoring. Biosens. Bioelectron. 54, 603–609.

Bariya, M., Nyein, H.Y.Y., Javey, A., 2018. Wearable sweat sensors. Nat. Electron. 1 (3), 160.

Brothers, M.C., DeBrosse, M., Grigsby, C.C., Naik, R.R., Hussain, S.M., Heikenfeld, J., Kim, S.S., 2019. Achievements and challenges for real-time sensing of analytes in sweat within wearable platforms. Acc. Chem. Res. 52 (2), 297–306.

Buono, M.J., Lee, N.V., Miller, P.W., 2010. The relationship between exercise intensity and the sweat lactate excretion rate. J. Physiol. Sci. 60 (2), 103–107.

Chung, M., Fortunato, G., Radacsi, N., 2019. Wearable flexible sweat sensors for healthcare monitoring: a review. J. R. Soc. Interface 16 (159), 20190217.

Coppedè, N., Giannetto, M., Villani, M., Lucchini, V., Battista, E., Careri, M., Zappettini, A., 2020. Ion selective textile organic electrochemical transistor for wearable sweat monitoring. Org. Electron. 78, 105579.

Curto, V.F., Fay, C., Coyle, S., Byrne, R., O'Toole, C., Barry, C., Hughes, S., Moyna, N., Diamond, D., Benito-Lopez, F., 2012. Real-time sweat pH monitoring based on a wearable chemical barcode micro-fluidic platform incorporating ionic liquids. Sensor. Actuator. B Chem. 171, 1327–1334.

Donaldson, S.H., Boucher, R.C., 2007. Sodium channels and cystic fibrosis. Chest 132 (5), 1631–1636.

Ferreira, P.C., Ataide, V.N., Chagas, C.L.S., Angnes, L., Coltro, W.K.T., Paixão, T.R.L.C., de Araujo, W.R., 2019. Wearable electrochemical sensors for forensic and clinical applications. Trac. Trends Anal. Chem. 119, 115622.

Gamella, M., Campuzano, S., Manso, J., de Rivera, G.G., López-Colino, F., Reviejo, A., Pingarrón, J., 2014. A novel non-invasive electrochemical biosensing device for in situ determination of the alcohol content in blood by monitoring ethanol in sweat. Anal. Chim. Acta 806, 1–7.

Gao, W., Emaminejad, S., Nyein, H.Y.Y., Challa, S., Chen, K., Peck, A., Fahad, H.M., Ota, H., Shiraki, H., Kiriya, D., 2016. Fully integrated wearable sensor arrays for multiplexed in situ perspiration analysis. Nature 529 (7587), 509–514.

Garcia-Cordero, E., Bellando, F., Zhang, J., Wildhaber, F., Longo, J., Guérin, H., Ionescu, A.M., 2018. Three-Dimensional integrated ultra-low-volume passive microfluidics with ion-sensitive field-effect transistors for multiparameter wearable sweat analyzers. ACS Nano 12 (12), 12646–12656.

Guinovart, T., Parrilla, M., Crespo, G.A., Rius, F.X., Andrade, F.J., 2013. Potentiometric sensors using cotton yarns, carbon nanotubes and polymeric membranes. Analyst 138 (18), 5208–5215.

Harris, R.C., Cohen, H.I., 1963. Sweat electrolytes in glycogen storage disease, type I. Pediatrics 31 (6), 1044–1046.

He, W., Wang, C., Wang, H., Jian, M., Lu, W., Liang, X., Zhang, X., Yang, F., Zhang, Y., 2019. Integrated textile sensor patch for real-time and multiplex sweat analysis. Sci. Adv. 5 (11), eaax0649.

Iguchi, S., Kudo, H., Saito, T., Ogawa, M., Saito, H., Otsuka, K., Funakubo, A., Mitsubayashi, K., 2007. A flexible and wearable biosensor for tear glucose measurement. Biomed. Microdevices 9 (4), 603–609.

Jeerapan, I., Sempionatto, J.R., Pavinatto, A., You, J.-M., Wang, J., 2016. Stretchable biofuel cells as wearable textile-based self-powered sensors. J. Mater. Chem. 4 (47), 18342–18353.

Jia, W., Bandodkar, A.J., Valdés-Ramírez, G., Windmiller, J.R., Yang, Z., Ramírez, J., Chan, G., Wang, J., 2013. Electrochemical tattoo biosensors for real-time noninvasive lactate monitoring in human perspiration. Anal. Chem. 85 (14), 6553–6560.

Karuppusamy, S., Babu, G.D., Venkatesh, V., Marken, F., Kulandainathan, M.A., 2017. Highly conductive nano-silver textile for sensing hydrogen peroxide. J. Electroanal. Chem. 799, 473–480.

Kim, J., Imani, S., de Araujo, W.R., Warchall, J., Valdés-Ramírez, G., Paixão, T.R., Mercier, P.P., Wang, J., 2015. Wearable salivary uric acid mouthguard biosensor with integrated wireless electronics. Biosens. Bioelectron. 74, 1061–1068.

Kim, J., Sempionatto, J.R., Imani, S., Hartel, M.C., Barfidokht, A., Tang, G., Campbell, A. S., Mercier, P.P., Wang, J., 2018. Simultaneous monitoring of sweat and interstitial fluid using a single wearable biosensor platform. Adv. Sci. 5 (10), 1800880.

Koh, A., Kang, D., Xue, Y., Lee, S., Pielak, R.M., Kim, J., Hwang, T., Min, S., Banks, A., Bastien, P., 2016. A soft, wearable microfluidic device for the capture, storage, and colorimetric sensing of sweat. Sci. Transl. Med. 8 (366), 366ra165-366ra165.

Lee, Y.-D., Chung, W.-Y., 2009. Wireless sensor network based wearable smart shirt for ubiquitous health and activity monitoring. Sensor. Actuator. B Chem. 140 (2), 390–395.

Li, X., Liu, X., 2016. A microfluidic paper-based origami nanobiosensor for label-free, ultrasensitive immunoassays. Adv. Healthcare Mater. 5 (11), 1326–1335.

Li, X., Liu, X.Y., 2014. Fabrication of three-dimensional microfluidic channels in a single layer of cellulose paper. Microfluid. Nanofluidics 16 (5), 819–827.

Li, X., Qin, Z., Fu, H., Li, T., Peng, R., Li, Z., Rini, J.M., Liu, X., 2021. Enhancing the performance of paper-based electrochemical impedance spectroscopy nanobiosensors: an experimental approach. Biosens. Bioelectron. 177, 112672.

Li, X., Zhao, C., Liu, X., 2015. A paper-based microfluidic biosensor integrating zinc oxide nanowires for electrochemical glucose detection. Microsyst. Nanoeng. 1, 15014.

Liu, H., Deng, J., 1995. An amperometric lactate sensor employing tetrathiafulvalene in nafion film as electron shuttle. Electrochim. Acta 40 (12), 1845–1849.

Lmberis, A., Dittmar, A., 2007. Advanced wearable health systems and applications-Research and development efforts in the European Union. IEEE Eng. Med. Biol. Mag. 26 (3), 29–33.

Luo, X., Shi, W., Yu, H., Xie, Z., Li, K., Cui, Y., 2018. Wearable carbon nanotube-based biosensors on gloves for lactate. Sensors 18 (10), 3398.

Mihali, C., Vaum, N., 2012. Use of plasticizers for electrochemical sensors. Recent Adv. Plasticizers 125.

Min, J., Sempionatto, J.R., Teymourian, H., Wang, J., Gao, W., 2020. Wearable electrochemical biosensors in North America. Biosens. Bioelectron. 172, 112750.

Mitsubayashi, K., Wakabayashi, Y., Murotomi, D., Yamada, T., Kawase, T., Iwagaki, S., Karube, I., 2003. Wearable and flexible oxygen sensor for transcutaneous oxygen monitoring. Sensor. Actuator. B Chem. 95 (1), 373–377.

Modali, A., Vanjari, S.R.K., Dendukuri, D., 2016. Wearable woven electrochemical biosensor patch for non-invasive diagnostics. Electroanalysis 28 (6), 1276–1282.

Morris, D., Coyle, S., Wu, Y., Lau, K.T., Wallace, G., Diamond, D., 2009. Bio-sensing textile based patch with integrated optical detection system for sweat monitoring. Sensor. Actuator. B Chem. 139 (1), 231–236.

Palleschi, G., Turner, A.P., 1990. Amperometric tetrathiafulvalene-mediated lactate electrode using lactate oxidase absorbed on carbon foil. Anal. Chim. Acta 234, 459–463.

Pantelopoulos, A., Bourbakis, N.G., 2010. A survey on wearable sensor-based systems for health monitoring and prognosis. IEEE Trans. Syst. Man Cybernet. Part C (Appl. Rev.) 40 (1), 1–12.

Pirovano, P., Dorrian, M., Shinde, A., Donohoe, A., Brady, A.J., Moyna, N.M., Wallace, G., Diamond, D., McCaul, M., 2020. A wearable sensor for the detection of sodium and potassium in human sweat during exercise. Talanta 219, 121145.

Possanzini, L., Decataldo, F., Mariani, F., Gualandi, I., Tessarolo, M., Scavetta, E., Fraboni, B., 2020. Textile sensors platform for the selective and simultaneous detection of chloride ion and pH in sweat. Sci. Rep. 10 (1), 1–14.

Promphet, N., Rattanawaleedirojn, P., Siralertmukul, K., Soatthiyanon, N., Potiyaraj, P., Thanawattano, C., Hinestroza, J.P., Rodthongkum, N., 2019. Non-invasive textile based colorimetric sensor for the simultaneous detection of sweat pH and lactate. Talanta 192, 424–430.

Rachoin, J.S., Weisberg, L.S., McFadden, C.B., 2010. Treatment of lactic acidosis: appropriate confusion. J. Hosp. Med. 5 (4), E1–E7.

Rathee, K., Dhull, V., Dhull, R., Singh, S., 2016. Biosensors based on electrochemical lactate detection: a comprehensive review. Biochem. Biophys. Rep. 5, 35–54.

Rosner, M.H., Kirven, J., 2007. Exercise-associated hyponatremia. Clin. J. Am. Soc. Nephrol. 2 (1), 151–161.

RoyChoudhury, S., Umasankar, Y., Jaller, J., Herskovitz, I., Mervis, J., Darwin, E., Hirt, P.A., Borda, L.J., Lev-Tov, H.A., Kirsner, R., 2018. Continuous monitoring of

wound healing using a wearable enzymatic uric acid biosensor. J. Electrochem. Soc. 165 (8), B3168–B3175.
Sahlin, K., 1986. Muscle fatigue and lactic acid accumulation. Acta Physiol. Scandinavica. Supplementum 556, 83–91.
Sempionatto, J.R., Jeerapan, I., Krishnan, S., Wang, J., 2020. Wearable chemical sensors: emerging systems for on-body analytical chemistry. Anal. Chem. 92 (1), 378–396.
Seshadri, D.R., Li, R.T., Voos, J.E., Rowbottom, J.R., Alfes, C.M., Zorman, C.A., Drummond, C.K., 2019. Wearable sensors for monitoring the physiological and biochemical profile of the athlete. NPJ Digital Med. 2 (1), 1–16.
Song, P., Wang, Y.-H., Liu, X., 2017. Flexible physical sensors made from paper substrates integrated with zinc oxide nanostructures. Flexible Printed Electron. 2 (3), 034001.
Tai, L.C., Gao, W., Chao, M., Bariya, M., Ngo, Q.P., Shahpar, Z., Nyein, H.Y., Park, H., Sun, J., Jung, Y., 2018. Methylxanthine drug monitoring with wearable sweat sensors. Adv. Mater. 30 (23), 1707442.
Wang, R., Zhai, Q., An, T., Gong, S., Cheng, W., 2021. Stretchable gold fiber-based wearable textile electrochemical biosensor for lactate monitoring in sweat. Talanta 222, 121484.
Wang, S., Bai, Y., Yang, X., Liu, L., Li, L., Lu, Q., Li, T., Zhang, T., 2020. Highly stretchable potentiometric ion sensor based on surface strain redistributed fiber for sweat monitoring. Talanta 214, 120869.
Windmiller, J.R., Wang, J., 2013. Wearable electrochemical sensors and biosensors: a review. Electroanalysis 25 (1), 29–46.
Wolfe, S., Cage, G., Epstein, M., Tice, L., Miller, H., Gordon Jr., R., 1970. Metabolic studies of isolated human eccrine sweat glands. J. Clin. Invest. 49 (10), 1880.
Yang, Y., Song, Y., Bo, X., Min, J., Pak, O.S., Zhu, L., Wang, M., Tu, J., Kogan, A., Zhang, H., Hsiai, T.K., Li, Z., Gao, W., 2020. A laser-engraved wearable sensor for sensitive detection of uric acid and tyrosine in sweat. Nat. Biotechnol. 38 (2), 217–224.
Yao, H., Liao, Y., Lingley, A., Afanasiev, A., Lähdesmäki, I., Otis, B., Parviz, B., 2012. A contact lens with integrated telecommunication circuit and sensors for wireless and continuous tear glucose monitoring. J. Micromech. Microeng. 22 (7), 075007.
Yilmaz, N.D., 2018. Nanocomposites for smart textiles. Smart Textiles: Wearable Nanotechnol. 211–245.
Yu, Y., Nyein, H.Y.Y., Gao, W., Javey, A., 2020. Flexible electrochemical bioelectronics: the rise of in situ bioanalysis. Adv. Mater. 32 (15), 1902083.
Zhai, Q., Yap, L.W., Wang, R., Gong, S., Guo, Z., Liu, Y., Lyu, Q., Wang, J., Simon, G.P., Cheng, W., 2020. Vertically aligned gold nanowires as stretchable and wearable epidermal ion-selective electrode for noninvasive multiplexed sweat analysis. Anal. Chem. 92 (6), 4647–4655.
Zhang, Y., Ram, M.K., Stefanakos, E.K., Goswami, D.Y., 2012. Synthesis, characterization, and applications of ZnO nanowires. J. Nanomater. 2012, 20.
Zhou, Z., Padgett, S., Cai, Z., Conta, G., Wu, Y., He, Q., Zhang, S., Sun, C., Liu, J., Fan, E., Meng, K., Lin, Z., Uy, C., Yang, J., Chen, J., 2020. Single-layered ultra-soft washable smart textiles for all-around ballistocardiograph, respiration, and posture monitoring during sleep. Biosens. Bioelectron. 155, 112064.